

# MODEL-BASED GENERATION OF NEUTRON INDUCED FISSION YIELDS UP TO 20 MEV BY THE GEF CODE

**K. Kern\*, M. Becker, C. Broeders and R. Stieglitz**

Institute for Neutron Physics and Reactor Technology

KIT Campus Nord, Hermann-von-Helmholtz-Platz 1, 76344 Leopoldshafen, Germany

[kilian.kern@kit.edu](mailto:kilian.kern@kit.edu)

[maarten.becker@kit.edu](mailto:maarten.becker@kit.edu)

[cornelis.broeders@kit.edu](mailto:cornelis.broeders@kit.edu)

[robert.stieglitz@kit.edu](mailto:robert.stieglitz@kit.edu)

## ABSTRACT

Model-based fission product yields from the fission of various important target nuclides have been calculated for incident neutron energies up to 20 MeV, divided into a 77 energy group structure. The calculations have been performed with two versions of the GEF code, which have been externally coupled to TALYS-1.4. In this application, the TALYS-1.4 code calculates any pre-fission nucleon or gamma emission from the compound nucleus as well as the probabilities of excitation states at the time it undergoes fission. The obtained quantities, fully characterizing the fissioning nucleus, are then passed to GEF, which generates the corresponding primary fission product yields in a Monte Carlo calculation. Cumulative fission product yields have been calculated using these primary fission product yields together with evaluated radioactive decay data as input. The interim and final results from the modelling, i. e. cross-sections, independent and cumulative fission yields, have been compared to experimental data. Important results from this, as well as sensitivities and reliabilities of the models, are discussed in this paper. The objective of this work was to generate energy dependent fission product yields data to serve as a basis for further investigations on potential improvements of evaluated data for nuclear reactor applications, which are beyond the scope of this publication.

**Key Words:** fission product yields, incident neutrons, energy dependence, modelling, GEF code, TALYS code

## 1. INTRODUCTION

The objective of this work, carried out in the context of a PhD work at KIT, is to generate neutron induced fission product yields in a fine energy group structure by up-to-date nuclear model codes, with the results being applied in further investigations of possible improvements in reactor physics calculations. Model-based fission product yields from the fission of various important target nuclides have been calculated by the nuclear fission model code GEF [1], which has been externally coupled to the general purpose nuclear reaction code TALYS-1.4 [2]. GEF is a development of K.-H. Schmidt and B. Jurado on behalf of the OECD NEA; TALYS is being developed at the NRG in

---

\*Corresponding author.

Petten, Netherlands, and the CEA in Bruyeres-le-Chatel, France. The GEF versions GEF-2012/2.3 and GEF-2013/2.2 have been applied with some minor changes, which will be discussed below. Calculations have been performed for incident neutron energies  $E_n$  up to 20 MeV, also requiring a proper modelling of pre-fission reactions which has been done by TALYS-1.4. For the obtained fission product yields, an energy group structure of 77 groups with boundaries being a subset of the 350 energy group boundaries applied by the reactor physics code KANEXT [3] for deterministic neutron flux calculations has been chosen. Issues to be investigated concerning fission product yields data have been discussed in an earlier publication [4]. As a first point, these involve the sensitivities of the effective fission product yields expressed by  $\bar{y}(A, Z, I)$  in (1) to the neutron flux spectrum  $\varphi(E_n)$ . The purpose of the fine calculation in 77 energy groups was to provide a reference solution for these energy weighted effective fission yields, from which the reproduction of their spectral dependencies by the coarse groups in state-of-the-art evaluated nuclear data can be examined. Secondly, it was found that the model applied for the completion of unmeasured “fractional independent yields” (i. e. the distribution of primary fission yields of single nuclides for a given mass expressed by  $f(A, Z, E_n)$  in (2)) in the generation of current evaluated fission yields data does not give a realistic description of even-odd effects in the yields depending on the proton number of the fission product. The factors  $Y(A, E_n)$  and  $R(A, Z, I, E_n)$  in (2) denote the yield as a function of fission product mass and the isomeric ratio.

$$\bar{y}(A, Z, I) = \frac{\int_0^\infty dE_n y(A, Z, I, E_n) \cdot \sigma_f(A, Z, I, E_n) \cdot \varphi(E_n)}{\int_0^\infty dE_n \sigma_f(A, Z, I, E_n) \cdot \varphi(E_n)} \quad (1)$$

$$y(A, Z, I, E_n) = Y(A, E_n) \cdot f(A, Z, E_n) \cdot R(A, Z, I, E_n) \quad (2)$$

$$\sum_Z f(A, Z, E_n) = 1 \qquad \sum_I R(A, Z, I, E_n) = 1$$

As a further field of application, the fission product yields generated in this work serve as a basis for the calculation of decay radiation, especially delayed neutron emission and decay heat, which is however additionally dependent on radioactive decay data. The improvement of fission yields modelling is motivated by the fact that it represents a step towards a physically consistent generic evaluation connecting a number of different quantities, which are cross-sections, fission product yields, prompt and delayed neutron emission as well as the prompt and delayed heat generation related to the fission process. In this paper the obtained energy-dependent fission product yields, the steps taken for their improvement and possible future work to improve the quality and consistency of the modelling are discussed.

## 2. APPLIED NUCLEAR REACTION MODELS

The general-purpose nuclear reaction model code TALYS-1.4 and two versions of the fission model code GEF have been applied in this work. A description of TALYS-1.4 is given in [5]. Within this

code, optical model calculations of reaction and shape-elastic scattering cross-sections are done by the integrated ECIS-06 code [6]. Nuclear reactions are classified into direct, pre-equilibrium and compound reactions, with the exciton model [7] and the Hauser-Feshbach formalism [8] describing the latter two important types in this application. The entire deexcitation process is tracked down by the code until the ground state or a metastable state is reached, with all possible decay channels out of gamma, neutron, proton, deuteron, triton, helion and alpha emission automatically being taken into account. Fission transmission coefficients are calculated by the Hill-Wheeler approach (exact solution assuming the fission barrier to be an inverted parabola) by default or by the Wentzel-Kramers-Brillouin (WKB) method as an alternative. As generally required, the fission model takes account of the multi-humped structure of the fission barrier. This means that a combined transmission coefficient is calculated for a barrier consisting of an inner and an outer hump with a deep minimum in between, however with only one fission channel being considered (single-mode). By default, the empirical barrier parameters from RIPL-3 [9] are applied as far as available, or they are calculated by a back-up model. A nuclear level density with transition from constant temperature to Fermi gas characteristics is applied by default. Detailed production cross-sections for emitted particles and residual nuclides are calculated as final result. In this work, the quantities of interest are the multi-chance fission probabilities and fission excitation functions calculated by the code, i. e. the probability for the excited nucleus to have a proton  $Z$  and neutron number  $N$ , an excitation energy  $E^*$  and a spin/parity state  $J^\pi$  right at the time it undergoes fission. This probability will be referred to as “fission contribution” below. TALYS-1.4 has been extended in this work to print it out into tables within an additional output file, from which the GEF input files are generated.

The GEF code is a semi-empirical fission model code calculating parent independent fission product yields and other observables related to the fission process. In this work, the versions GEF-2012/2.3 and GEF-2013/2.2 have been applied. The code calculates the weights of the different fission channels by the ratios of the Hill-Wheeler penetrabilities of outer fission barriers, with fission barrier and level density parameters being determined by analytical formulae. In the newer version GEF-2013/2.2, the impact of the inner fission barrier is additionally considered, which plays a role in the fission of transuranium nuclides. GEF considers up to four or five fission channels (multi-mode), which is necessary for fission yields modelling, since pre-neutron fission fragment mass distribution is described as a superposition of Gaussians with the respective fission channel weight; for the standard-II channel it is in fact a folding of a Gaussian with a box function which better represents the experimental data. The widths of the fragment mass distributions are determined by a semi-empirical description as a function of the fissioning system and its excitation energy. In the GEF model it is assumed that the fragment mass distribution is fixed when the system passes the outer fission barrier, whereas the fragment  $\frac{N}{Z}$  ratio is determined later at the scission point. This is justified by calculations based on the Langevin equation of motion, which showed a large inertia for the mass division [10] and a small inertia for the  $\frac{N}{Z}$  degree of freedom [11] during the fission process. Thus, the mean  $\frac{N}{Z}$  ratio is determined by a scission point model for a given mass division, taking an empirical tip distance between the fragments as well as their quadrupole deformations as input. For this scission point configuration, the potential energy is minimized with respect to the  $\frac{N}{Z}$  ratio of the fragments, and another empirical shift is added to this so-called “charge polarization” to take account of nuclear shell effects. As for the width of the mass distribution, there is a similar description for the width of the  $\frac{N}{Z}$  distribution of pre-neutron fractional independent fission yields. Excitation energies are treated as intrinsic excitation, collective excitation and deformation energy. In the description of the division of excitation energies among the two fission fragments, the nascent fragments are treated as individual interacting nuclei with their own nuclear temperature, with the

intrinsic excitation energy flowing to the colder fragment. This corresponds to the application of the so-called “separability principle” [12]. It is assumed that the superfluid phase transition occurring in the fragments leads to a constant nuclear temperature up to a total intrinsic excitation energy of 13 MeV, which results in an excitation energy division different from the one expected by the Fermi gas model, according to which the intrinsic excitation energy is divided proportionally to the mass numbers. The code treats several even-odd effects: Firstly, the even-odd effect of pre-neutron fission fragment yields as a function of their  $Z$  and  $N$ , which is related to the mentioned flow of excitation energy as well as nucleon pairing effects [13]. Secondly, the newer version GEF-2013/2.2 also includes the even-odd effect of the total excitation energy (TXE) depending on the division of proton numbers among the fission fragments. The need to include the latter effect is discussed in [14]. Fission fragment deexcitation by neutron and gamma emission represents the final important step in the physical modelling of fission product yields. In the GEF code, this is done by a spin independent Weisskopf-Ewing [15] calculation, which however has been observed to give good results for the prompt neutron emission. To take the competition between neutron and gamma emission into account, analytical expressions for the decay widths  $\Gamma_n(A, Z, E^*)$  and  $\Gamma_\gamma(A, Z, E^*)$  from [16, 17] are applied. The calculation of isomeric ratios of the fission product yields is based on the mean spin value calculated for the corresponding pre-neutron fission fragments. This value is determined by their moment of inertia perpendicular to the fission axis, their excitation energy and nuclear temperature, an additional even-odd effect depending on their proton number and, of course, the spin value  $J_{CN}$  of the fissioning nucleus.

In this work, both versions of the GEF code have been extended by an empirical description of ternary fission (i. e. into three fragments) in order to obtain the yields of light fission products like  $^4\text{He}$  or  $^3\text{H}$  originating from this process. The description of the ratio of ternary fission to total fission follows the references [18, 19]. It typically has a value around 0.2%. Relative yields of light ternary fragments as well as the interplay of their emission with the properties of the other two medium-weight fragments are described by systematics, according to experimental observations to be found in the same sources. The excitation energy of the light ternary fission fragments was assumed to be zero.

Another modification applied to the GEF-2012/2.3 code involved the dependence of the mean fragment masses from a specific fission channel on the excitation energy of the fissioning nucleus. It has been observed that the mean masses of the mass-asymmetric standard-I and standard-II channels shift towards  $\frac{A_{CN}}{2}$  if the excitation energy is increased [14], as indicated in Figure 1. This mean mass shift, as included in all newer GEF versions, was added to GEF-2012/2.3 and led to an overall improvement in the energy dependencies of fission product yields from the model calculation, especially in the tails of the mass distribution.

In the original GEF code, the excitation energy  $E_{CN}^*$  of the compound nucleus is determined by a formula similar to (3), and the nucleus is assumed to undergo fission without prior nucleon or gamma emission. The original version may therefore only be used below the second-chance fission threshold, where this approximation is acceptable. For the compound nucleus spin  $J_{CN}$ , the spin value of the target is taken. In this work,  $E_{CN}^*$  and  $J_{CN}$  have been replaced by the values calculated by TALYS-1.4, along with the  $Z_{CN}$  and  $A_{CN}$  of the different fissioning nuclei resulting from possible pre-fission nucleon emission. The weights of the fission channels, however, are still determined by GEF.

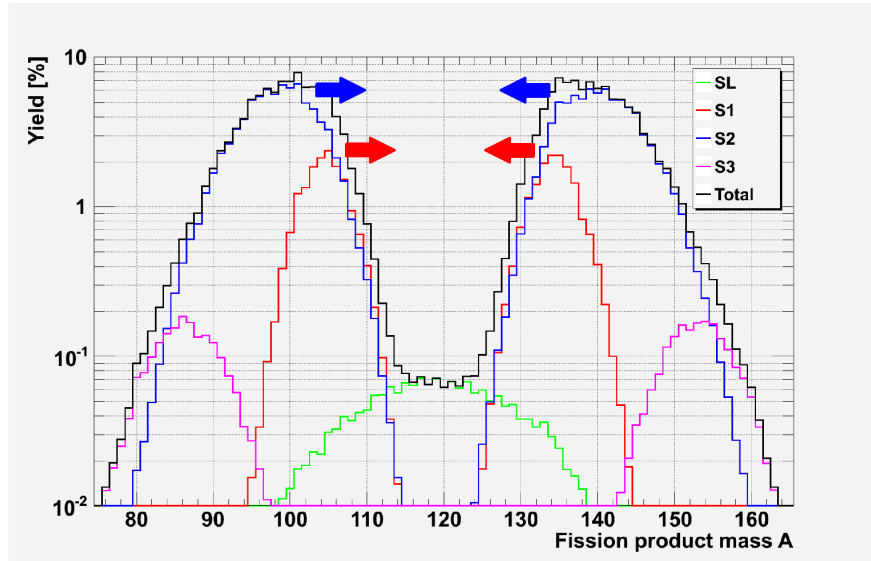


**Figure 1.** The mean masses of the mass-asymmetric standard-I (S1) and standard-II (S2) fission channels shift towards  $\frac{A_{CN}}{2}$  when  $E_{CN}^*$  increases (schematic figure).

### 3. MODELLING OF PRE-FISSION PROCESSES

#### 3.1. Application of TALYS-1.4 Code

The task of TALYS-1.4 in this work was to calculate the fission contribution for a given incident neutron energy. Immediately after neutron capture, the nucleus is in its initial excitation state with the excitation energy given by (3), with the neutron and compound nucleus masses  $m_n$  and  $m_{CN}$  and the neutron separation energy  $S_n$ . Prior to fission, as the excitation state of the nucleus allows, nucleons and excitation energy may be lost mainly by neutron and gamma emission. Thus, for first-chance fission, i. e. without nucleon loss prior to fission, the probability distribution for the excitation energy at fission consists of a discrete component representing the direct (n, f) and a continuum representing the (n,  $\gamma$ f) processes, as illustrated in Figure 2.

$$E_{CN,i}^* = \left(1 - \frac{m_n}{m_{CN}}\right) \cdot E_n + S_n(Z_{CN}, A_{CN}) \quad (3)$$

The TALYS-1.4 calculations of the fission contribution were carried out for 237 incident neutron energy values from  $E_n = 74.4$  eV to  $E_n = 19.95$  MeV with a maximum energy step of  $\Delta E_n \leq 100$  keV. In each calculation, the continuum of the fission contribution was divided into 100 energy bins, whereas the discrete component from the binary (n, f) reactions was treated separately. The TALYS-1.4 outputs were subsequently condensed into the 77 group structure for the fission yields. There are in fact fluctuations of the fission yields occurring at the epithermal resonances of the fission cross-section [20–22], which would require an even finer treatment than in this work, but for which a theoretical modelling based on the resonance parameters is not yet available. The neglect

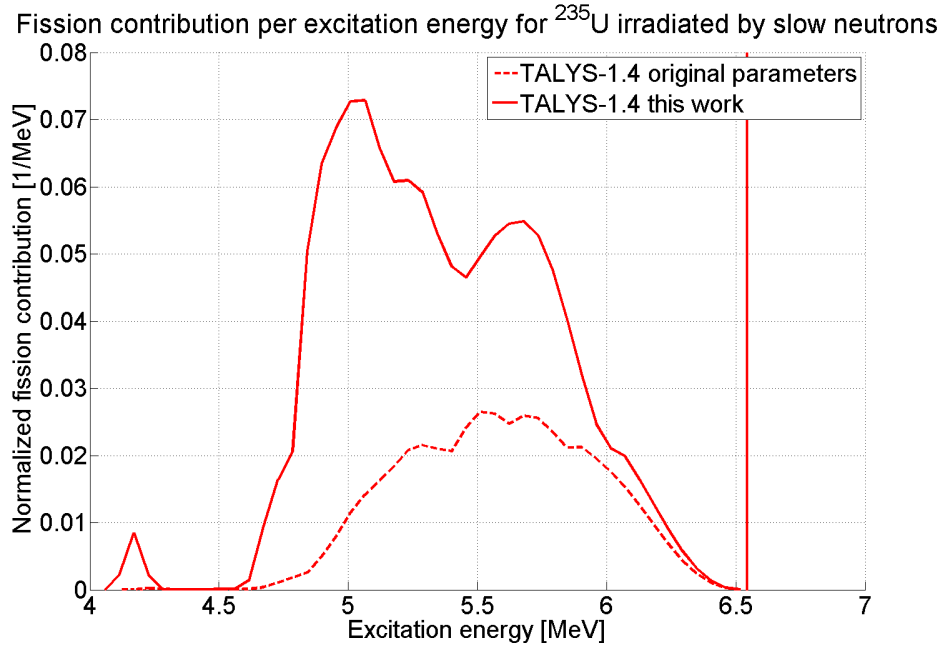


**Figure 2.** Fission contribution per excitation energy unit for the compound nucleus  $^{236}\text{U}$  formed by slow neutron irradiation of  $^{235}\text{U}$ , calculated by TALYS-1.4 with original parameters from [23] and improved parameters from the TASMANT-1.51 application in this work. It consists of a discrete component at  $E_{\text{CN}}^* = 6.5455$  MeV and a continuum. The integral has been normalized to one.

of microscopic resonance effects also represents the main limitation of TALYS when applied to low neutron energies. To better resolve the energy range  $E_n < 1.1100 \cdot 10^5$  eV, where the fission rate is very high in many cases, it was divided more finely into five groups, with the upper boundaries of the three lowest ones being at  $E_n = 1.4873 \cdot 10^2$  eV,  $E_n = 2.2395 \cdot 10^3$  eV and  $E_n = 1.5030 \cdot 10^4$  eV.

In this work, the results from TALYS-1.4 calculations with default model parameters were found to be poor, especially concerning the agreement of the  $^{232}\text{Th}$  and  $^{238}\text{U}$  fission cross-sections with experimental data. The calculations were repeated with fitted model parameters provided by [23]. Further optimizations of the input parameters for  $^{233}\text{U}$  and  $^{235}\text{U}$  could be achieved in this work by the application of the TASMANT-1.51 code [24]. This code optimizes selected input parameters by a simplex algorithm, calculating the loss function from experimental data sets either for a single target or for multiple targets. The latter option is supposed to give a consistent fit of the parameters for all targets, which is however beyond the scope of this work. As shown in Figure 2, the weight of  $(n, \gamma f)$  processes in total fission has changed considerably by this parameter adjustment, nevertheless the direct  $(n, f)$  processes are still dominating. Generally, one should be aware of the uncertainties originating from the modelling of the fission contribution.

Fission barrier transmission coefficients have been calculated by the Hill-Wheeler approach for single-mode fission, taking into account the resonances originating from class-II excitation states in the potential well between the inner and outer fission barrier. Many important fission barrier parameters were set in the input, with the remainder being taken from RIPL-3 [9] as far as available, or calculated by the Sierk model [25] as back-up. For a similar number of fission barriers, the parameters of the level density on top of the barrier have also been adjusted. The fact that the

TALYS-1.4 model assumes fission to occur through only one channel, with the weights of the multiple fission channels being required for fission yields modelling and determined later on by GEF, represents an inconsistency in the modelling. It could be resolved e. g. by the application of the TALYS alternative EMPIRE-3.2 [26], which supports the calculation of fission transmission coefficients by the multi-mode approach. However, this would also increase the number of fission barrier parameters to be fitted.

All level density parameters have been taken from systematics. The impact of collective effects (i. e. excitation energy being bound in rotation or vibration instead of intrinsic excitations) on the level density has been described by an effective treatment instead of explicit enhancement factors. In this effective treatment, a phenomenological energy dependency of the parameter  $a$  in the Fermi gas level density formula is applied. This takes account of the vanishing of collective effects with increasing excitation energy and has, according to [5], so far been more successful in the description of fission cross-sections. Notably, most of the improvement of the fission cross-sections of  $^{233}\text{U}$  and  $^{235}\text{U}$  has been reached by limiting the number of collective rotational excited states being included in the coupled-channels calculation to two instead of five. This change affected the calculation of the total cross-section, which led to an improvement of the total cross-section itself as well as the fission cross-section at incident neutron energies below about 2 MeV.

### 3.2. Experimental Validation of Results

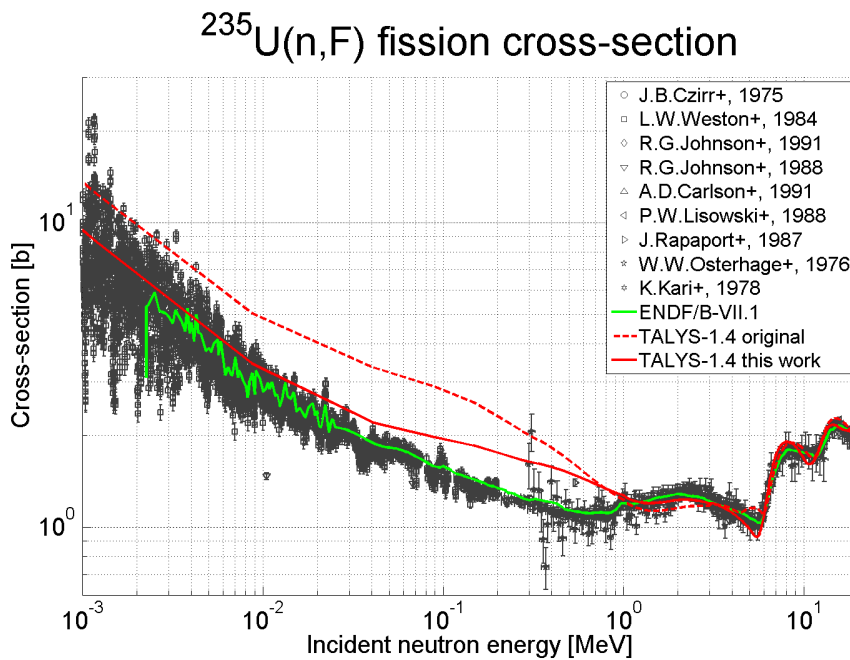


**Figure 3.** Fission cross-section of  $^{235}\text{U}$  for incident neutrons in the energy range  $1 \text{ keV} \leq E_n \leq 20 \text{ MeV}$  from TALYS-1.4 calculations, evaluated and experimental data.

In order to validate the TALYS-1.4 calculations, the cross-sections for fission, capture, inelastic scattering, neutron multiplication as well as the total cross-section have been compared to experimental data. Figure 3 shows the fission cross-section of  $^{235}\text{U}$  from the TALYS-1.4 calculations

once with original parameters from [23] and once with parameters from this work, together with the ENDF/B-VII.1 evaluation [27] and experimental data retrieved from the EXFOR database [28].

A general improvement of the total and fission cross-section of  $^{235}\text{U}$  below 2 MeV has been achieved. There is still a deviation of the calculated fission cross-section from the experimental data at  $10\text{ keV} \leq E_n \leq 1\text{ MeV}$ . For the target  $^{233}\text{U}$ , such a deviation did not remain after the TASMANT-1.51 application. However, there is not a large impact of the cross-sections in this energy range on the final GEF results, since the excitation energy of the discrete (n, f) component in Figure 2, which was found to contribute over 90% to the total fission in this range, is not affected by the model variations. Instead, sensitivities of the final results on the TALYS calculation were rather observed above the (n, nf) second-chance fission threshold. It must be noted that the fission cross-section is only an integral quantity resulting from the fission contribution, which cannot be directly verified by experiment and thus relies on good modelling. Only for the nucleon loss preceding fission, there are indications from the yields and angular correlations of particles emitted in the fission process.

## 4. CALCULATION OF FISSION PRODUCT YIELDS

### 4.1. Application of GEF Code

In this work, the two versions GEF-2012/2.3 and GEF-2013/2.2 have been modified as described above and coupled to TALYS-1.4. The statistical fluctuations of variables and deexcitation cascades of fission fragments are all calculated by Monte Carlo methods. For each of the 77 energy groups, the values of the parent independent fission product yields were determined by a single calculation with  $5 \cdot 10^7$  fission events. The number of events calculated for each bin of the fission contribution was proportional to the probability of the respective fissioning nucleus and excitation state, and the results were summed up. The calculation with GEF-2013/2.2 was supplemented by a calculation of the fission yield covariance matrix for each energy group, taking into account the systematical and statistical uncertainties from the GEF code. Compared with the former, the latter type of uncertainties are negligible for the yields displayed in Figures 4-6. For the determination of the covariance matrix,  $N = 224$  runs with each about  $2.23 \cdot 10^5$  events have been performed for each group. At the beginning of each run, 22 of the GEF model parameters were varied independently according to their estimated uncertainties as given in the original GEF-2013/2.2. The covariance matrix  $V$  was then obtained by (4) from the yields  $y_{i,k}$  calculated in each run  $k$  and their mean values  $\bar{y}_i$ .

$$V_{ij} = \frac{1}{N} \cdot \sum_{k=1}^N (y_{i,k} - \bar{y}_i) \cdot (y_{j,k} - \bar{y}_j) \quad (4)$$

### 4.2. Calculation of Cumulative Fission Product Yields

A new external code for the calculation of the cumulative fission product yields, which represent the independent fission product yield plus the integral yield from the decay of mother nuclides, has

been developed in this work. It calculates the cumulative yields  $c_i$  from the independent ones by the recursion (5), with  $P_{ji}$  the decay branching ratio from nuclide  $j$  to nuclide  $i$ . For the primary fission products most far from stability, it holds  $\sum_j P_{ji} \cdot c_j = 0$ . As generally usual, nuclides with half lives of more than 1000 years have been considered as “stable” in this context. The uncertainties of the cumulative yields, as shown in Figures 5 and 6, have been calculated by (6), thus neglecting the covariances of the independent fission yields and of the decay data.

$$c_i = y_i + \sum_j P_{ji} \cdot c_j \quad (5)$$

$$\sigma_{c_i} = \sqrt{\sigma_{y_i}^2 + \sum_j \left( c_j^2 \cdot \sigma_{P_{ji}}^2 + P_{ji}^2 \cdot \sigma_{c_j}^2 \right)} \quad (6)$$

The code reads the radioactive decay data, i. e. the  $P_{ji}$ ,  $\sigma_{P_{ji}}$  and decay half lives, from an ENDF-6 file. In this work, the ENDF/B-VII.1 radioactive decay data library [27] has been applied. It must be noted that the uncertainty information on the file is incomplete, and that some technical errors had to be corrected for this calculation, involving multiple listings of the same daughter nuclide and isomer in decay branching ratios as well as extremely long decay half-lives being set to zero.

### 4.3. Experimental Validation of Results

The fission product yields being compared to experimental data in this section originate from the following model calculations: Firstly, the coupling of TALYS-1.4 with GEF-2012/2.3 including the above mentioned code modifications, and secondly the coupling of TALYS-1.4 with the newer GEF-2013/2.2. The TALYS-1.4 calculations have been carried out with the optimized parameters obtained from the TASMAN-1.51 application. Results for the target  $^{235}\text{U}$  are presented. In this work, the calculation results have been compared to experimental data from the EXFOR database [28] considering the following aspects:

- Independent single-nuclide yields from thermal neutron induced fission, with particular respect to nuclide yields that have been measured at the Lohengrin spectrometer at ILL Grenoble [29] and the OSIRIS facility at Studsvik [30], but without information on the isomeric state of the fission products in this case. These data are important and enable the validation of the code, independent from radioactive decay data. See Figure 4.
- Cumulative single-nuclide yields from thermal neutron induced fission, with particular respect to delayed neutron precursors far from stability. Experimental data have been obtained from Rudstam et al. [30]. Beyond the scope of this publication, the modelling of delayed neutron emission represents one further application of this work. See Figure 5.
- Cumulative single-nuclide yields from high energetic neutrons around 14.7 MeV, where a number of experiments [31–36] are available, to validate the code at high neutron energies. See Figure 6.

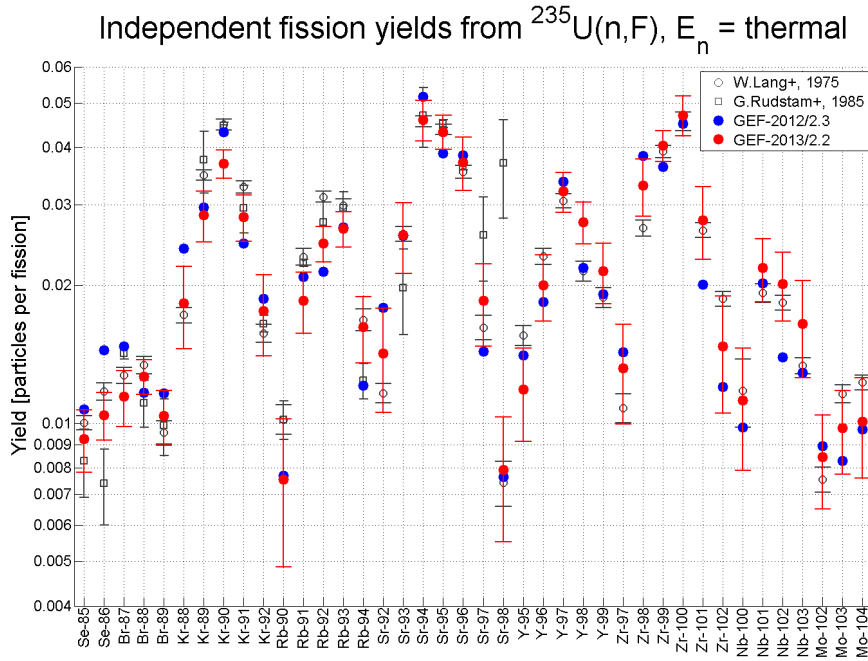


**Figure 4.** Parent independent fission product yields from  $^{235}\text{U}(n,F)$  ( $E_n = \text{thermal}$ ) calculated in this work, compared to experimental data from [29, 30], without information on isomeric states. Error bars denote the  $1\sigma$  uncertainty of experimental data and GEF-2013/2.2 results.

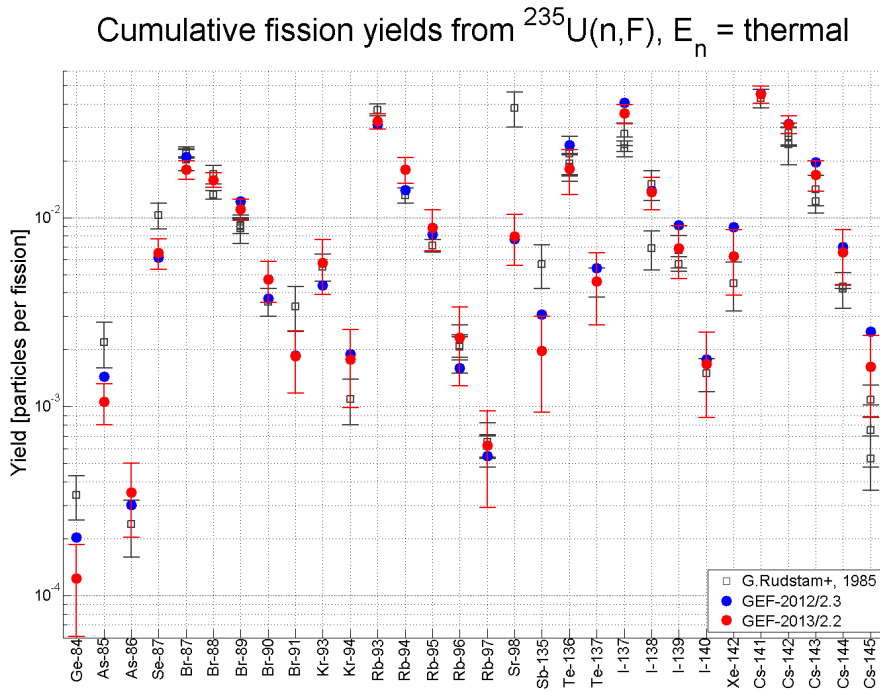


**Figure 5.** Parent cumulative fission product yields from  $^{235}\text{U}(n,F)$  ( $E_n = \text{thermal}$ ) calculated in this work, compared to experimental data from [30]. All displayed nuclides are in their ground state. Error bars denote the  $1\sigma$  uncertainty of experimental data and GEF-2013/2.2 results.

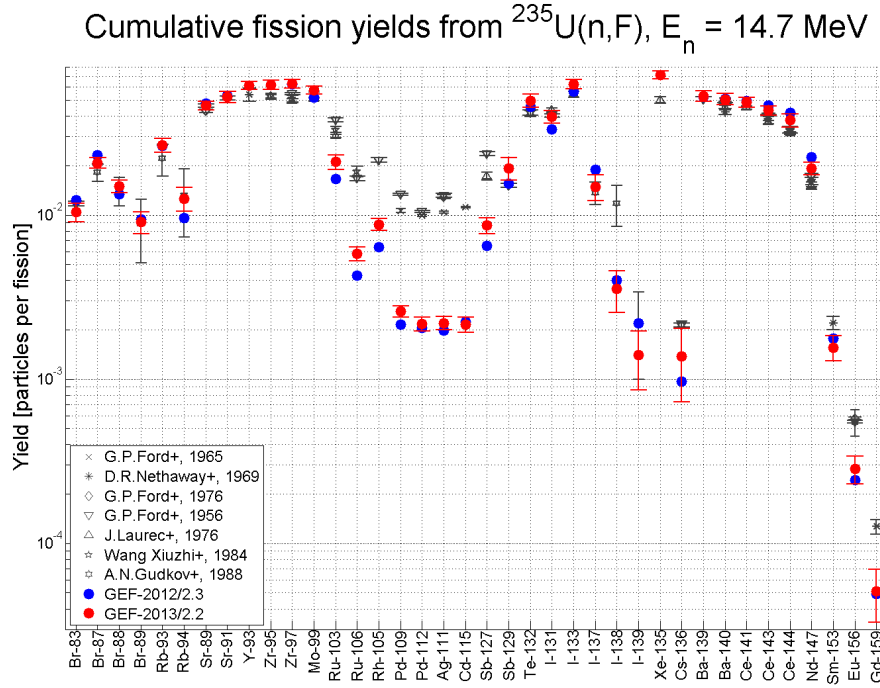


**Figure 6.** Parent cumulative fission product yields from  $^{235}\text{U}(n,F)$  ( $E_n = 14.7$  MeV) calculated in this work, compared to experimental data from [31–36]. All displayed nuclides are in their ground state. Error bars denote the  $1\sigma$  uncertainty of experimental data and GEF-2013/2.2 results.

To measure the quality of the model-based yields, a test quantity  $H$  given by (7) has been calculated as proposed in [37], with  $N$  the number of experimental data points. Another quantity  $\tilde{H}$  has been introduced in this work to evaluate the uncertainties obtained from GEF-2013/2.2. Both  $H$  and  $\tilde{H}$  are calculated by a sum of the squares of residuals, normalized by their expected variance for the respective hypothesis. The hypothesis behind (7) is that the model reproduces the true values exactly, whereas the hypothesis behind (8) is that the true value is within the calculated model uncertainty. In the ideal case when both hypotheses are true, it holds  $\sigma_{y_i^{\text{calc}}} = 0$  and  $H = \tilde{H} \approx 1$  if the  $\sigma_{y_i^{\text{exp}}}$  values are correct. If only the second hypothesis is true,  $H > \tilde{H} \approx 1$  is expected. The  $1\sigma$  confidence interval of the test quantities has been calculated from the related  $\chi^2$  distribution. All values are given in Table I.

$$H = \sqrt{\frac{1}{N} \cdot \sum_{i=1}^N \frac{(y_i^{\text{exp}} - y_i^{\text{calc}})^2}{\sigma_{y_i^{\text{exp}}}^2}} \quad (7)$$

$$\tilde{H} = \sqrt{\frac{1}{N} \cdot \sum_{i=1}^N \frac{(y_i^{\text{exp}} - y_i^{\text{calc}})^2}{\sigma_{y_i^{\text{exp}}}^2 + \sigma_{y_i^{\text{calc}}}^2}} \quad (8)$$

The values of  $H$  in Table I obtained for GEF-2013/2.2 are lower than for GEF-2012/2.3 in all three cases, showing an improvement in the modelling. Given the fact that there seems to be an

**Table I.** Values of  $N$ ,  $H$  and  $\tilde{H}$  for Figures 4-6.

Figure	$N$	$H, \tilde{H}$	$H$	$H$	$\tilde{H}$
		$1\sigma$ confidence interval	GEF-2012/2.3	GEF-2013/2.2	GEF-2013/2.2
4	60	0.913 - 1.097	4.52	3.50	1.12
5	51	0.906 - 1.106	5.10	3.98	1.26
6	69	0.919 - 1.090	21.97	20.83	11.20

error in the experimental data for  $^{98}\text{Sr}$  from [30], the value of  $\tilde{H}$  for the independent yields from GEF-2013/2.2 in Figure 4 is acceptable, indicating a realistic estimation of model uncertainties. The model uncertainties in Figure 5 seem to be slightly underestimated. However, high values of  $H$  and  $\tilde{H}$  have been obtained for the  $E_n = 14.7$  MeV fission, where the modelled yields in the “valley” region around  $\frac{A_{\text{CN}}}{2}$  are too low by a factor of five and deviate far beyond the error limits. The deviations observed in Figure 6 are mainly caused by a wrong description of the weight of the superlong (SL) fission channel.

## 5. CONCLUSIONS

One general conclusion is that there is certainly room and motivation for further development. Concerning the GEF code, it has become clear that some issues need to be resolved. As observed here, these involve the weight of the superlong channel at high energy fission. It is suggested to resolve this by changing the empirical correction to the height of the outer fission barrier for this channel. As found in this work, the estimation of uncertainties by GEF-2013/2.2 seems to work well e. g. for thermal fission of  $^{235}\text{U}$ , but given the fact that the amount of empirical information is different from case to case, it is probably not yet appropriate for all targets and incident energies and needs more refinements. The results from this work suggest that a larger uncertainty should be assumed for the outer fission barrier height of the superlong channel of the fissioning nuclei  $^{235}\text{U}$  and  $^{234}\text{U}$ , which play a role in irradiation of  $^{235}\text{U}$  by 14.7 MeV neutrons. There has been an improvement of the calculation results with the switch from GEF-2012/2.3 to GEF-2013/2.2, mainly related to the improved description of the neutron even-odd effect in the fission product yields. As found in more detailed analyses beyond the scope of this publication, the reproduction of fission yield energy dependencies for the target  $^{235}\text{U}$  has been found to be satisfactory for the vast majority of nuclides at incident energies at least up to  $E_n = 5$  MeV. This indicates the applicability of the model to calculations of effective fission yields in fission reactors, as discussed in the introduction.

In this work, a model-based covariance matrix of parent independent fission yields has been obtained, which could be valuable e. g. for future evaluations of nuclear data and other purposes. Fission yield covariances are so far not available in evaluated data libraries. However, it must be noted that the assessment of uncertainties and covariances in this field is still at an early stage. In this work, the uncertainties originating from TALYS-1.4 as well as the error correlations in the calculation of cumulative fission yields have been neglected. This may have led to an incorrect estimation of uncertainties in Figure 5 and especially Figure 6.

The strength of the nuclear reaction modelling in this work is that it utilizes physically sound models not only to reproduce experimental fission yields data, but also being based on the fit of model parameters to experimental cross-section data, thus well exploiting the available experimental database. However, the predictive power of this modelling has also been found to be limited. There are still inconsistencies in the modelling, especially between the single-mode description of fission in the TALYS code and the multi-mode description in GEF, which could be resolved e. g. by an application of EMPIRE-3.2 as proposed. Work on this and on the further application of the model-based fission yields data, as discussed in the introduction, is in progress.

## ACKNOWLEDGMENTS

This work has been performed at the Institute for Neutron Physics and Reactor Technology (INR) of the Karlsruhe Institute of Technology (KIT). The authors would like to thank the Program Nuclear Safety Research of KIT for the financial support of the research topic “Multi-Physics Methods for LWR.” Thanks also to K.-H. Schmidt for the lively collaboration and to A. Koning for providing the TASMANT-1.51 code and the TALYS input files for this work.

## REFERENCES

- [1] K.-H. Schmidt, B. Jurado, “Global view on fission observables - new insights and new puzzles,” *Proceedings of GAMMA-1*, JRC-IRMM and University of Novi Sad, Novi Sad, Serbia, November 22-24, 2011, *Physics Procedia* **31** (editor S. Oberstedt), pp. 147-157, <http://dx.doi.org/10.1016/j.phpro.2012.04.020> (2012)
- [2] A. J. Koning, S. Hilaire, M. C. Duijvestijn, “TALYS-1.0,” *Proceedings of the International Conference on Nuclear Data for Science and Technology*, CEA, Nice, France, April 22-27, 2007, EDP Sciences (editors O. Bersillon *et al.*), pp. 211-214, <http://dx.doi.org/10.1051/ndata:07767> (2008)
- [3] M. Becker, S. Van Criekingen, C. H. M. Broeders, “KANEXT, a tool for nuclear reactor calculations,” Institute for Neutron Physics and Reactor Technology, Karlsruhe Institute of Technology, <http://inrwww.webarchiv.kit.edu/kanextExport.html> (2010)
- [4] K. Kern, M. Becker, C. Broeders, “Assessment of fission product yields data needs in nuclear reactor applications,” *Proceedings of PHYSOR 2012*, ANS, Knoxville, Tennessee, USA, April 15-20, 2012, [http://inrwww.webarchiv.kit.edu/students\\_work/k\\_kern\\_physor\\_2012.html](http://inrwww.webarchiv.kit.edu/students_work/k_kern_physor_2012.html) (2012)
- [5] A. J. Koning, S. Hilaire, S. Goriely, “TALYS-1.4 User Manual,” NRG, Petten, Netherlands, <http://www.talys.eu/fileadmin/talys/user/docs/talys1.4.pdf> (2011)
- [6] J. Raynal, “Notes on ECIS94,” *CEA Saclay Reports*, **CEA-N-2772** (1994)
- [7] A. J. Koning, M. C. Duijvestijn, “A global pre-equilibrium analysis from 7 to 200 MeV based on the optical model potential,” *Nuclear Physics A*, **744**: pp. 15-76, <http://dx.doi.org/10.1016/j.nuclphysa.2004.08.013> (2004)

- [8] W. Hauser, H. Feshbach, "The Inelastic Scattering of Neutrons," *Physical Review*, **87**: pp. 366-373, <http://dx.doi.org/10.1103/PhysRev.87.366> (1952)
- [9] R. Capote *et al.* "RIPL - Reference Input Parameter Library for Calculation of Nuclear Reactions and Nuclear Data Evaluations," *Nuclear Data Sheets*, **110**: pp. 3107-3214, <http://dx.doi.org/10.1016/j.nds.2009.10.004> (2009)
- [10] G. D. Adeev, V. V. Pashkevich, "Theory of macroscopic fission dynamics," *Nuclear Physics A*, **502**: pp. 405-422, [http://dx.doi.org/10.1016/0375-9474\(89\)90679-9](http://dx.doi.org/10.1016/0375-9474(89)90679-9) (1989)
- [11] A. V. Karpov, G. D. Adeev, "Langevin description of charge fluctuations in fission of highly excited nuclei," *European Physical Journal A*, **14**: pp. 169-178, <http://dx.doi.org/10.1140/epja/i2002-10004-2> (2002)
- [12] K.-H. Schmidt, A. Kelic, M. V. Ricciardi, "Experimental evidence for the separability of compound-nucleus and fragment properties in fission," *Europhysics Letters*, **83**: 32001, <http://dx.doi.org/10.1209/0295-5075/83/32001> (2008)
- [13] K.-H. Schmidt, B. Jurado, "Further evidence for energy sorting from the even-odd effect in fission-fragment element distributions," arXiv:1007.0741v2, <http://arxiv.org/abs/1007.0741v2> (2013)
- [14] K. Kern, *Investigations on the build-up and impacts of fission products in nuclear fast reactors*, diploma thesis, Institute for Neutron Physics and Reactor Technology, Karlsruhe Institute of Technology, [http://inrwww.webarchiv.kit.edu/students\\_work/k\\_kern.html](http://inrwww.webarchiv.kit.edu/students_work/k_kern.html) (2011)
- [15] V. F. Weisskopf, D. H. Ewing, "On the Yield of Nuclear Reactions with Heavy Elements," *Physical Review*, **57**: pp. 472-485, 935, <http://dx.doi.org/10.1103/PhysRev.57.472>, <http://dx.doi.org/10.1103/PhysRev.57.935.2> (1940)
- [16] Th. Rubehn *et al.* "Scaling laws in  $^3\text{He}$  induced nuclear fission," *Physical Review C*, **54**: pp. 3062-3067, <http://dx.doi.org/10.1103/PhysRevC.54.3062> (1996)
- [17] A. V. Ignatyuk, "Systematics of low-lying level densities and radiative widths," *Proceedings of Bologna 2000: Structure of the Nucleus at the Dawn of the Century*, Joint University of Bologna - INFN, Bologna, Italy, May 29 - June 3, 2000, World Scientific (editors G. C. Bonsignori *et al.*), Vol. 3, pp. 287-292, [http://dx.doi.org/10.1142/9789812810922\\_0053](http://dx.doi.org/10.1142/9789812810922_0053) (2001)
- [18] I. Halpern, "Three fragment fission," *Annual Review of Nuclear and Particle Science*, **21**: pp. 245-294, <http://dx.doi.org/10.1146/annurev.ns.21.120171.001333> (1971)
- [19] C. Wagemans, *The Nuclear Fission Process*, CRC Press, Boca Raton, Florida, USA (1991)
- [20] F.-J. Hamsch, H.-H. Knitter, C. Budtz-Jorgensen, "Fission mode fluctuations in the resonances of  $^{235}\text{U}(n,f)$ ," *Nuclear Physics A*, **491**: pp. 56-90, [http://dx.doi.org/10.1016/0375-9474\(89\)90206-6](http://dx.doi.org/10.1016/0375-9474(89)90206-6) (1989)

- [21] J. Frehaut, D. Shackleton, “Mesure du nombre moyen de neutrons prompts et de l’énergie moyenne des rayons gamma prompts emis lors de la fission induite par neutrons de resonance dans  $^{235}\text{U}$  et  $^{239}\text{Pu}$ ,” *Proceedings of Third IAEA Symposium on the Physics and Chemistry of Fission*, IAEA, Rochester, NY, USA, August 13-17, 1973, INDC Special 1 STI/PUB/347, Vol. II, pp. 201-210, <https://www-nds.iaea.org/publications/tecdocs/sti%252Fpub%252F0347-vol2/> (1974)
- [22] R. E. Howe, T. W. Phillips, C. D. Bowman, “Prompt fission neutrons from eV resonances in  $^{235}\text{U}$ : Measurement and correlation with other fission properties,” *Physical Review C*, **13**: pp. 195-205, <http://dx.doi.org/10.1103/PhysRevC.13.195> (1976)
- [23] A. J. Koning, private communication (2013)
- [24] A. J. Koning, D. Rochman, “Modern Nuclear Data Evaluation with the TALYS Code System,” *Nuclear Data Sheets*, **113**: pp. 2841-2934, <http://dx.doi.org/10.1016/j.nds.2012.11.002> (2012)
- [25] A. J. Sierk, “Macroscopic model of rotating nuclei,” *Physical Review C*, **33**: pp. 2039-2053, <http://dx.doi.org/10.1103/PhysRevC.33.2039> (1986)
- [26] M. Herman *et al.* “EMPIRE: Nuclear Reaction Model Code System for Data Evaluation,” *Nuclear Data Sheets*, **108**: pp. 2655-2715, <http://dx.doi.org/10.1016/j.nds.2007.11.003> (2007)
- [27] M. B. Chadwick *et al.* “ENDF/B-VII.1 Nuclear Data for Science and Technology: Cross Sections, Covariances, Fission Product Yields and Decay Data,” *Nuclear Data Sheets*, **112**: pp. 2887-2996, <http://dx.doi.org/10.1016/j.nds.2011.11.002> (2011)
- [28] O. Schwerer, “EXFOR Formats Description for Users (EXFOR Basics),” *Documentation Series of the IAEA Nuclear Data Section*, **IAEA-NDS-206**, [https://www-nds.iaea.org/nrdc/nrdc\\_doc/](https://www-nds.iaea.org/nrdc/nrdc_doc/) (2008)
- [29] W. Lang *et al.* “Nuclear charge and mass yields for  $^{235}\text{U}(n_{\text{th}}, f)$  as a function of the kinetic energy of the fission products,” *Nuclear Physics A*, **345**: pp. 34-71, [http://dx.doi.org/10.1016/0375-9474\(80\)90411-X](http://dx.doi.org/10.1016/0375-9474(80)90411-X) (1980)
- [30] G. Rudstam *et al.* “Yields of Products from Thermal Neutron-Induced Fission of  $^{235}\text{U}$ ,” *Radiochimica Acta*, **49**: pp. 155-192, <http://www.degruyter.com/view/j/ract.1990.49.issue-4/ract.1990.49.4.155/ract.1990.49.4.155.xml?format=INT> (1990)
- [31] G. P. Ford, R. B. Leachman, “Fission Mass Yield Dependence on Angular Momentum,” *Physical Review*, **137**: pp. B826-B836, <http://dx.doi.org/10.1103/PhysRev.137.B826> (1965)
- [32] D. R. Nethaway, B. Mendoza, T. E. Voss, “Low-Yield Products from Fission of  $^{232}\text{Th}$ ,  $^{235}\text{U}$ , and  $^{238}\text{U}$  with 14.8-MeV Neutrons,” *Physical Review*, **182**: pp. 1251-1259, <http://dx.doi.org/10.1103/PhysRev.182.1251> (1969)
- [33] G. P. Ford, A. E. Norris, “A compilation of yields from neutron-induced fission of  $^{232}\text{Th}$ ,  $^{235}\text{U}$ ,  $^{236}\text{U}$ ,  $^{237}\text{Np}$ ,  $^{238}\text{U}$ , and  $^{239}\text{Pu}$  measured radiochemically at Los Alamos,” *Los Alamos Scientific Lab. Reports*, **LA-6129** (1976)

- [34] J. Laurec *et al.* “Fission Product Yields of  $^{233}\text{U}$ ,  $^{235}\text{U}$ ,  $^{238}\text{U}$  and  $^{239}\text{Pu}$  in Fields of Thermal Neutrons, Fission Neutrons and 14.7-MeV Neutrons,” *Nuclear Data Sheets*, **111**: pp. 2965-2980, <http://dx.doi.org/10.1016/j.nds.2010.11.004> (2010)
- [35] Wang Xiuzhi, Li Ze, “The absolute determination of cumulative yield of several nuclides from 14.9 MeV neutron-induced fission of U-235,” *He Huaxue yu Fangshe Huaxue*, **6**: p. 229 (1984)
- [36] A. N. Gudkov *et al.* “Yields of Delayed Neutron Precursors in the Fission of Actinides,” *Radiochimica Acta*, **57**: pp. 69-76, <http://www.degruyter.com/view/j/ract.1992.57.issue-2-3/ract.1992.57.23.69/ract.1992.57.23.69.xml?format=INT> (1992)
- [37] A. Yu. Konobeev *et al.* “What Can We Expect from the Use of Nuclear Models Implemented in MCNPX at Projectile Energies below 150 MeV? Detailed Comparison with Experimental Data,” *Proceedings of the International Conference on Nuclear Data for Science and Technology*, Korean Nuclear Society and KAERI, Jeju Island, South Korea, April 26-30, 2010, Journal of Korean Physical Society, Vol. 59, pp. 927-930, <http://dx.doi.org/10.3938/jkps.59.927> (2011)